The Sensitivity of Atmospheric Correction of Reflectances to the Surface BRDF

Baoxin Hu, Wolfgang Wanner, Xiaowen Li, Alan H. Strahler

(*Department of Geography and Center for Remote Sensing, Boston University, 725 Commonwealth Avenue, Boston, MA 02215, USA, Tel.* +1-617-353-5981, *Fax* +1-617-353-3200, *e-mail baoxin/wanner/lix/alan@crsa.bu.edu*)

Abstract This paper systematically studies the relationship between surface BRDF (Bidirectional Reflectance Distribution Function) retrieval and atmospheric correction. The study uses the atmospheric correction scheme of the Moderate Resolution Imaging Spectroradiometer (MODIS), and angular sampling expected for MODIS and MISR (Multiangle Imaging Spectro-Radiometer) for different land cover types and optical depths of aerosols. The results show that it is necessary to consider the surface anisotropic BRDF in atmospheric correction, and surface BRDF retrieval and atmospheric correction can be coupled in a converging iteration loop.

Key words Atmospheric correction, BRDF, MODIS

1 INTRODUCTION

Most objects have anisotropic reflectances, which can be described by the bidirectional reflectance distribution function (BRDF). In remote sensing applications, the surface BRDF can only be retrieved from remotely sensed data after the removal of atmospheric effects. But performing atmospheric correction in turn requires the knowledge of the surface reflectance properties. To resolve this interdependency, some atmospheric correction methods assume that the surface is Lambertian. The atmospheric correction scheme of the Moderate Resolution Imaging Spectroradiometer (MODIS)[1] couples atmospheric correction and the surface BRDF retrieval by performing an iteration loop. In this scheme, atmospheric correction is first performed on MODIS observations under the assumption of an isotropic surface BRDF; the reflectances are then used to retrieve a new BRDF; atmospheric correction is updated based on the new BRDF.

The important question for these atmospheric correction methods is whether it is necessary to take surface anisotropic reflectance properties into consideration in atmospheric correction and how to do that. Here we will systematically analyze the relationship between surface BRDF retrieval and atmospheric correction based on the atmospheric correction scheme of MODIS[1].

2 THEORETICAL BASIS AND SIMULATION DATA

In the atmospheric correction algorithm for MODIS[1], the reflectance at the top of the atmosphere for the visible and near-infrared bands are expressed as

$$\rho_{toa} = \rho_0 + e^{-\tau/\mu_v} e^{-\tau/\mu_s} \rho_s + e^{-\tau/\mu_v} t_d(\mu_s) \bar{\rho} + e^{-\tau/\mu_v} t_d(\mu_v) \bar{\rho}' + t_d(\mu_s) t_d(\mu_v) \bar{\bar{\rho}} + \frac{(e^{-\tau/\mu_s} + t_d(\mu_s))(e^{-\tau/\mu_v} + t_d(\mu_v)) S (\bar{\bar{\rho}})^2}{1 - S\bar{\bar{\rho}}} \quad (1)$$

where ρ_{toa} is the reflectance at the top of the atmosphere; ρ_0 is the intrinsic atmospheric reflectance; ρ_s is the surface reflectance; S is the reflectance of the atmosphere for isotropic light entering the base of the atmosphere; μ_s is the cosine of the solar zenith angle, and μ_v is the cosine of the view zenith angle; $e^{-\tau/\mu_s}$ and $t_d(\mu_s)$ are the downward direct and diffuse transmittance of the atmosphere along the path of the incoming solar beam, respectively; $e^{-\tau/\mu_v}$ and $t_d(\mu_v)$

are the upward direct and diffusive transmittance of the atmosphere in the viewing direction, respectively; τ is the atmospheric optical depth; $\bar{\rho}$, $\bar{\rho}'$ and $\bar{\bar{\rho}}$ are the surface hemispherical-directional, directional-hemispherical, and hemispherical-hemispherical reflectances, respectively. These reflectances depend on both atmospheric optical parameters and surface reflectance properties. See [1] for their full definitions. In a dynamic mode, to account for changes in land cover, equation (1) is modified as follows:

$$\rho_{toa} = \rho_0 + e^{-\tau/\mu_v} e^{-\tau/\mu_s} \rho_s + \rho_s [e^{-\tau/\mu_v} t_d(\mu_s) \bar{\rho}^* + e^{-\tau/\mu_s} t_d(\mu_v) \bar{\rho}'^* + t_d(\mu_s) t_d(\mu_v) \bar{\bar{\rho}}^* + \rho_s \frac{(e^{-\tau/\mu_s} + t_d(\mu_s))(e^{-\tau/\mu_v} + t_d(\mu_v)) S (\bar{\bar{\rho}}^*)^2}{1 - S\bar{\bar{\rho}}}] \quad (2)$$

$$\bar{\rho}^* = \frac{\bar{\rho}}{\rho_s^m}, \quad \bar{\rho}'^* = \frac{\bar{\rho}'}{\rho_s^m}, \quad \bar{\bar{\rho}}^* = \frac{\bar{\bar{\rho}}}{\rho_s^m}, \quad (3)$$

where, ρ_s^m is a predicted surface reflectance, for example taken from a BRDF model. If we have such a predicted BRDF, ρ_s^m, and from it the coupling terms, $\bar{\rho}$, $\bar{\rho}'$ and $\bar{\bar{\rho}}$, ρ_s can be obtained by solving equation (2). As we mentioned above, the problem is how to obtain the BRDF-dependent parameters.

When the surface is Lambertian, $\bar{\rho}^* = \bar{\rho}'^* = \bar{\bar{\rho}}^* = 1$ and $\bar{\bar{\rho}} = \rho_s$ Thus, equation (2) can be simplified as

$$\rho_{toa} = \rho_0 + \frac{(e^{-\tau/\mu_s} + t_d(\mu_s))(e^{-\tau/\mu_v} + t_d(\mu_v))\rho_s}{1 - S\rho_s} \quad (4)$$

So, under the assumption of a Lambertian, ρ_s can easily be calculated using equation (4).

In this study, we use the forward mode of 6S[2] to calculate simulated observation data (ρ_{toa}) of MODIS and MISR using equation (1), under the following simulation conditions:

1) Angular sampling. We use the angular samplings of MODIS and MISR for geographic locations from latitude 60° south (-60°) to latitude 60° north (+60°) at intervals of 15° during a 16-day period around March 12.

2) Surface cover types. Four typical land cover types are analyzed here. These are a plowed field, a hard wheat field with 11 percent of vegetation coverage, a grass lawn (vegetation coverage: 97%; LAI: 9.9) and a hardwood forest. Their bidirectional reflectances are calculated by Ambrals (Algorithm for Modis Bidirectional Reflectance Anisotropics of the Land Surface)[3]. The model parameters for these land cover types in the red and near-infrared bands are determined by fitting Ambrals to the corresponding field-measured data sets[4-6].

3) Atmospheric conditions. The simulated atmospheric conditions are for a continental aerosol model and aerosol optical depths at 550nm of 0.1, 0.2 and 0.4.

3 SENSITIVITY OF RETRIEVED SURFACE REFLECTANCE TO THE INPUT SURFACE REFLECTANCE PROPERTIES

From equation (2), one can see that the surface BRDF enters atmospheric correction through $\bar{\rho}^*$, $\bar{\rho}'^*$ and $\bar{\bar{\rho}}^*$. To obtain the relationship between atmospheric correction and surface BRDF retrieval, we investigate the sensitivity of the retrieved surface reflectance to these ratios. Assuming that an error occurs $\bar{\rho}^*$, $\bar{\rho}'^*$ or $\bar{\bar{\rho}}^*$, such as 1%, we calculate the root mean square error (rmse) caused in the retrieved surface reflectances for a given angular sampling. The results based on all cases studied are shown in Fig. 1.

In Fig. 1, the x-axis shows the relative errors (%) in the input $\bar{\rho}^*$, $\bar{\rho}'^*$ or $\bar{\bar{\rho}}^*$; the y-axis shows the mean rmse (%) between the true surface reflectances and the retrieved values, caused by the errors in $\bar{\rho}^*$, $\bar{\rho}'^*$ or $\bar{\bar{\rho}}^*$. The error bars show the range of the rmse in the cases investigated (different land cover types and latitudes). From these plots, we can see that: 1). the retrieved surface reflectance is more sensitive to $\bar{\rho}^*$ and $\bar{\rho}'^*$ than to $\bar{\bar{\rho}}^*$; 2). with increasing optical depth of aerosols, the sensitivity of the retrieved reflectance to $\bar{\rho}^*$, $\bar{\rho}'^*$ and $\bar{\bar{\rho}}^*$ increases. Based on these results, we analyze the relationship between atmospheric correction and surface BRDF retrieval by considering two kinds of atmospheric correction methods.

Lambertian-based atmospheric correction

Lambertian-based atmospheric correction assumes the surface is Lambertian, where $\bar{\rho}^*$, $\bar{\rho}'^*$ and

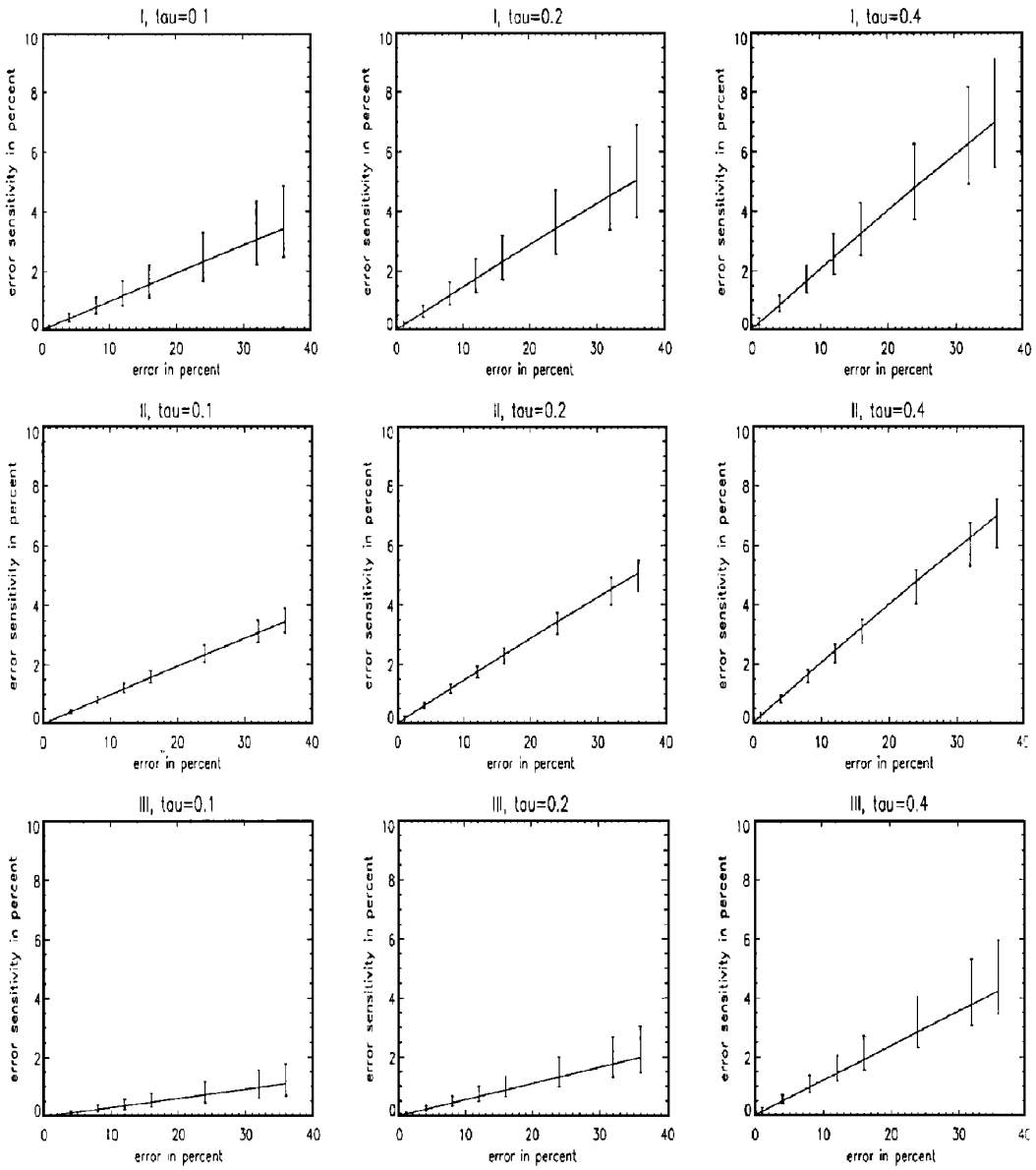

Fig·1 The sensitivity of the retrieved surface reflectances to $\bar{\rho}^*$ (I), $\bar{\rho}'^*$ (II), and $\bar{\bar{\rho}}^*$ (III) in the red band

$\bar{\bar{\rho}}^*$ equal 1. We calculate the rmse in $\bar{\rho}^*$, $\bar{\rho}'^*$ and $\bar{\bar{\rho}}^*$ caused by this assumption for a given simulated MODIS/MISR 16-day angular sampling. Column III of Table 1 shows the mean rmses of all cases (different latitudes and land cover types) for $\bar{\rho}^*$, $\bar{\rho}'^*$ and $\bar{\bar{\rho}}^*$, and their range (in brackets). Referring to Fig. 1, we can see that these errors in $\bar{\rho}^*$, $\bar{\rho}'^*$ and $\bar{\bar{\rho}}^*$ can lead to large errors in the retrieved surface reflectance. For example, when the aerosol optical depth is 0.1, the mean error caused in the retrieved surface reflectance is 3.2% in the red band, and the

Table 1 The rmse (%) in $\bar{\rho}^*$, $\bar{\rho}'^*$ and $\bar{\bar{\rho}}^*$ in the red band

		Lambertian assumption	BRDF
$\bar{\rho}^*$	τ=0.1	13.42(7.06—27.68)	2.09(0.77—5.66)
	τ=0.2	12.35(6.31—26.86)	2.78(1.00—7.84)
	τ=0.4	11.99(6.19—27.92)	4.08(1.51—11.82)
$\bar{\rho}'^*$	τ=0.1	13.35(6.99—28.50)	1.85(0.62—5.97)
	τ=0.2	12.10(6.00—26.83)	2.56(0.89—8.32)
	τ=0.4	11.58(5.59—26.88)	4.02(1.51—12.13)
$\bar{\bar{\rho}}^*$	τ=0.1	23.91(14.34—56.53)	2.95(1.11—8.24)
	τ=0.2	23.91(14.34—56.53)	4.15(1.65—12.17)
	τ=0.4	23.91(14.34—56.53)	6.99(2.84—19.02)

error ranges from 1.8% to 7.7%. This can be demonstrated by the results of carrying out a Lambertian-based atmospheric correction.

We perform a Lambertian-based atmospheric correction to the ρ_{toa} calculated above using the inverse mode of 6S according to equation (4). Table 2 shows the rmse (%) between the true surface reflectances and the retrieved values from this Lambertian-based atmospheric correction, and its standard deviation (in brackets) based on all cases investigated here. From this table, we can note that assuming a Lambertian surface causes a large error in the retrieved surface reflectance. Meanwhile, the large deviation indicates that the size of the error varies with the surface BRDF shape. The farther away from isotropy the BRDF shape, the larger the error made. From the above analysis, we can see that one should take the surface BRDF into account in atmospheric correction.

The coupled BRDF retrieval and atmospheric correction iteration loop

The first step of the loop consists of using Ambrals to fit the reflectances retrieved from the Lambertian-based atmospheric correction to obtain the Ambrals BRDF model parameters. Based on these model parameters and the atmospheric optical parameters, the estimated $\bar{\rho}^*$, $\bar{\rho}'^*$ and $\bar{\bar{\rho}}^*$ can be calculated. Then atmospheric correction of ρ_{toa} is performed. This atmospheric correction method we call BRDF-based atmospheric correction. The mean rmses in $\bar{\rho}^*$, $\bar{\rho}'^*$ and $\bar{\bar{\rho}}^*$ shown in column IV of Table 1 are much smaller than those caused by a Lambertian assumption. Based on Fig. 1, we find that these errors in $\bar{\rho}^*$, $\bar{\rho}'^*$ and $\bar{\bar{\rho}}^*$ cause acceptably small errors with the mean value of 0.5% in the retrieved reflectances, for a nonturbid atmosphere. But when the optical depth of aerosols is 0.4, the error in the retrieved reflectance is still larger, ranging from 0.8% to 9.1% and with the mean value of 2.7%. These points are also demonstrated by the rmse between the true surface reflectances and the retrieved values from the first step of the coupled BRDF retrieval and atmospheric correction iteration loop (see column II of the Table 2).

Table 2 The rmse(%) between the true BRDF and the retrived BRDF

walelength	τ=0.1		τ=0.2		τ=0.4	
	I	II	I	II	I	II
red	3.24(1.45)	0.51(0.41)	4.77(2.21)	1.08(0.81)	7.45(3.72)	2.63(1.83)
nir	1.95(0.77)	0.17(0.11)	3.12(1.28)	0.44(0.30)	5.01(2.35)	1.25(0.83)

τ: the optical depth of aerosols at 550nm; I: Lambertian-based atmosperic correction;
II: the first step of the coupled atmospheric correction and surface BRDF retrieval loop

To investigate if the iteration loop converges, we iteratively perform the loop several times. For every step, we use Ambrals to fit the reflectances retrieved from the last step and do BRDF-based atmospheric correction based on the inversion results. The rmse between the true surface reflectances and the retrieved values, and the relative change in the model parameters between the adjacent steps, decrease as more iterations are performed. Thus the loop of coupled surface BRDF retrieval and atmospheric correction converges. For a turbid atmosphere, we are required to perform the iteration loop more than one time. In our study, when the optical depth of aerosols is 0.4, two steps are already sufficient to obtain a mean error of only 0.89% in the retrieved reflectances in the red band.

4 CONCLUSIONS

We analyze the sensitivity of the retrieved surface refectance to the surface reflectance properties assumed. From the results, we draw the following conclusions: 1) Even for a non-turbid atmosphere, the assumption of a Lambertian surface in atmospheric correction causes large errors in the retrieved surface reflectances. For example, when the aerosol optical

depth is 0.1, the error ranges from 1.7% to 7.6% in the red band. Thus, it is necessary to consider the surface anisotropic BRDF in atmospheric correction. 2) Surface BRDF retrieval and atmospheric correction can be coupled in an converging iteration loop, which improves the quality of atmospheric correction and of subsequent BRDF retrieval.

ACKNOWLEDGEMENTS

This work is supported by NASA under contract NAS 5-31369, and partly by NNSF of China under grant 49331020.

REFERENCE

[1] Vermote, E. F., *et al*. Logorithm Technical background Document: Atmospheric Correction Algorithm. odis Science Team and Associates, 1995.

[2] Vermote, E. *et al*. Econd Simulation of the Satellite Signal in the Solar Spectrum (6S). S User Guide Version 0, NASA-Goddard Space Flight Center-Code 923, Greenbelt, MD 20771, 1994.

[3] Strahler, A. H., *et al*. ODIS BRDF/ Albedo Product: Algorithm Theoretical Basis Document Version 3.2. NASA EOS-MODIS, 1995.

[4] Kimes, D. S., A. G. Kerber, P. J. Seller. Dynamics of directional reflectance factor distribution for vegetation canopies. *Appl. Opt.*, 1983, **22**(9): 1,364—1,372.

[5] Kimes, D. S., W. W. Newcomb, C. J. Tucker, *et al*. Directional reflectance factor distributions for cover types of Northern Africa. *Remote Sens. Environ.*, 1985, **18**: 1—19.

[6] Kimes, D. S., W. W. Newcomb, R. F. Nelson, J. B. Schutt. Directional reflectance distributions of a hardwood and a pine forest canopy. *IEEE Trans. Geosci. Remote Sens.*, 1986, **24**: 281—293.

AUTHOR

Hu Baoxin, obtained B. S. and M. S. from Department of Electric Engineering, Tianjing University in 1987 and 1990 respectively. Now she is currently a Ph. D. student jointly advised by faculties of IRSA, China, and at Boston University's Center for Remote Sensing and Department of Geography, USA. She is working on advanced methods in the investigation of surface and atmospheric scattering.

表面 BRDF 反射率大气纠正的敏感度分析

胡宝新, Wolfgang Wanner, 李小文, Alan H. Strahler

(*Department of Geography and Center for Remote Sensing, Boston University, 725 Commonwealth Avenue, Boston, MA 02215, USA*)

摘　要　该文系统地研究了 BRDF 反演和大气纠正的关系。研究中用到了 MODIS 的大气纠正法，而且，对于不同的植被类型和气溶胶光学深度用到了 MODIS 和 MISR 的角度采样。结果显示在大气纠正中考虑 BRDF 表面各向异性是必要的，而且表面 BRDF 的反演和大气纠正可以迭代进行，大量模拟证明这一迭代收敛迅速。

关键词　大气纠正，二向性反射分布函数，MODIS